Role of Microtubules in Polarized Delivery of Apical Membrane Proteins to the Brush Border of the Intestinal Epithelium

Christian Achler, David Filmer, Christa Merte, and Detlev Drenckhahn

Department of Anatomy and Cell Biology, University of Marburg, D-3550 Marburg, Federal Republic of Germany

Abstract. Colchicine- and vinblastine-induced depolymerization of microtubules (MTs) in the intestinal epithelium of rats and mice resulted in significant delivery of three apical membrane proteins (alkaline phosphatase, sucrase–isomaltase, and aminopeptidase N) to the basolateral membrane domain. In addition, typical brush borders (BBs) occurred at the basolateral cell surface, consisting of numerous microvilli that contained the four major components of the cytoskeleton of apical microvilli (actin, villin, fimbrin, and the 110-kD protein). Formation of basolateral microvilli required polymerization of actin and proceeded at glycocalyx-studded plaques that resembled the dense plaques located at the tips of apical microvilli. BBs from the basolateral membrane became internalized into BB-containing vacuoles which served as recipient organelles for newly synthesized apical membrane proteins. The BB vacuoles fused with each other and finally were inserted into the apical BB. Polarized distribution of Na^+,K^+-ATPase, a basolateral membrane protein, was not affected by drug-induced depolymerization of MTs. These observations indicate that Golgi-derived carrier vesicles (CVs) containing apical membrane proteins are vectorially guided to the apical cell surface by a retrograde transport along MTs. MTs are uniformly oriented towards a narrow space underneath the apical terminal web (termed subterminal space) that contains MT-organizing properties and controls polarized alignment of MTs. In contrast to apical CVs, targeting of basolateral CVs appears to be independent of MTs but demands a barrier at the apical membrane domain that prevents basolateral CVs from apical fusion (transport barrier hypothesis).

THE absorptive intestinal epithelium provides a typical example of a polarized cell layer. Its surface can be divided into two domains, the apical and the basolateral membrane domain which differ in structure and function (21, 32, 40). The surface area of the apical domain of the plasma membrane is increased severalfold by numerous microvilli which form the brush border (BB)[1] (5, 52). Each microvillus is supported by an axial core bundle of actin filaments that are extensively cross-linked by two proteins, villin (95,000 M_r) and fimbrin (68,000 M_r) (7, 13, 38). The core bundle end is inserted into electron dense material at the microvillus tip, which is studded with a conspicuous fuzzy glycocalyx (5, 40). Laterally, the actin filament bundle is connected to the microvillus membrane by rod-shaped bridging filaments that consist of a complex of the myosin-related 110-kD protein and calmodulin (7–9, 34, 38). The lateral epithelial cell surface is moderately increased by folds (40) that do not contain any significant amounts of the microvillar actin-binding proteins, villin, fimbrin, and the 110-kD protein (13, 14). Moreover, the apical and basolateral plasma membrane differ from each other by the presence of several specialized integral membrane proteins that are either restricted to the apical membrane (e.g., alkaline phosphatase, aminopeptidases, or disaccharidases) or to the basolateral membrane (e.g., Na^+,K^+-ATPase) (21, 26, 28, 32).

Thus far, there is still little information on how the polarized distribution of membrane proteins and the polarized cellular morphology is generated and how it is maintained. Several lines of evidence suggest that the Golgi apparatus (GA) and its associated *trans*-network plays an important role in the process of sorting the membrane proteins into different populations of vesicles that will be transported and inserted into either the apical or basolateral plasma membrane domain (11, 23, 33, 37, 46, 51). From experiments with microtubule (MT)-disrupting agents, it has been concluded that MTs are probably important for the vectorial transport of several apically destined membrane proteins from the GA towards the apical plasma membrane (3, 4, 12, 19, 27, 47).

To obtain further insight into the role of MTs in cellular

A preliminary report of this work was presented at the 83rd meeting of the Anatomische Gesellschaft in Zürich, Switzerland on March 20-23, 1988.

David Filmer's present address is Department of Biology, Purdue University, West Lafayette, Indiana.

1. *Abbreviations used in this paper*: BB, brush border; CV, carrier vesicle; GA, Golgi apparatus; MDCK, Madin–Darby canine kidney; MT, microtubule.

polarity, we have studied targeting of three apical and one basolateral membrane protein in the intestinal epithelium of rats and mice treated with the MT-depolymerizing drugs colchicine and vinblastine. These drugs have been recently shown to interfere with the polarized delivery of various ectoenzymes to the intestinal BB and to induce the formation of numerous finger-like projections at the basolateral plasma membrane, which eventually aggregate to form BB-like structures (3, 4, 12, 19, 27, 42, 43). It is currently unknown how these microvillus-like structures are formed and whether they contain the main molecular constituents which are normally restricted to the apical microvilli. Finally, by using the experimental approach of perturbing cellular polarity we hoped to find mechanisms that allow the cells to regain polarity.

Materials and Methods

Drug Treatment

Young adult rats (Hanover-Wistar strain) and mice (BALB/C) of both sexes were maintained on a ground chow (Altromin, Lage, FRG). All drugs were dissolved in 1 ml of the solutions indicated and administered by stomach tube (gavage). After overnight fasting (with free access to water), animals were treated with colchicine (52 rats, 13 mice) (Serva Feinbiochemica GmbH, Heidelberg, FRG) (10 mg/kg body weight) or vinblastine sulfate (five rats, three mice) (Lilly, Giessen, FRG) (15 mg/kg body weight) freshly dissolved in 1 ml of phosphate-buffered (20 mM) saline (125 mM) (PBS, pH 7.4). At various time intervals after application of the drugs, animals were anesthetized with ether and killed by cervical dislocation. Six rats received a second dose of colchicine at 6 or 12 h and were killed 1–6 h later. Control animals received either lumicolchicine (10 mg/kg) or PBS. Lumicolchicine was purchased from Sigma Chemical Co. (St. Louis, MO) or prepared by UV irradiation of colchicine. In a further series of experiments, 10 colchicine-treated rats received at 0 or 6 h a single dose of cycloheximide (14 mg/kg body weight, dissolved in PBS) (six rats) or cytochalasin D (2.5 μg/kg body weight, dissolved in DMSO) (four rats). The animals were killed 6 h later. Both drugs were from Sigma Chemical Co. Control animals received 1 ml PBS or DMSO, respectively, not containing drugs.

Electron Microscopy

Small pieces of duodenal mucosa were fixed for at least 2 h with 2% glutaraldehyde in PBS (pH 7.4). After several washes with PBS, tissue pieces were fixed afterward with 1% OsO_4 in PBS (1 h, 4°C), dehydrated in graded ethanol series, immersed with propylene oxide, and embedded in Epon 812. Ultrathin sections were counterstained with lead citrate and uranyl acetate, and examined with a Zeiss EM 10 electron microscope (Oberkochen, FRG) (14). Freeze fracture replicas were obtained from pieces of fixed duodenal mucosa immersed for 25 min in 5% glycerol, quick frozen in melting Freon 22 (113 K), cooled with liquid nitrogen, and fractured, etched, and shadowed with carbon and platinum as described elsewhere (6).

Antibodies and Immunocytochemistry

Preparation and specificity of affinity-purified rabbit antibodies against actin, villin, fimbrin, the 110-kD protein, and tubulin have been described in detail in previous studies (13, 15). Antibodies specific for rabbit intestinal sucrase-isomaltase (22) and aminopeptidase N (20) were the kind gifts of Dr. Semenza and Dr. Wacker (Dept. Biochemistry, Eidgenössische Technische Hochschule, Zürich, Switzerland), and Dr. Maroux (Dept. Biochemistry, CBM-CNRS, Marseille, France). Mouse antibodies against calf intestinal alkaline phosphatase were obtained from Dianova GmbH (Hamburg, FRG). Antibodies cross-reacting with antigens of the GA were obtained by immunizing mice (BALB/c) with various protein bands excised from SDS-PAGE of microsomes that were prepared from rat kidney outer medulla. One mouse which had been immunized with a 55-kD polypeptide band developed an antibody strongly reactive with the GA of various epithelial cells including rat intestinal epithelium. As determined by immunoblotting, the antibody cross-reacted with two polypeptide bands at 55 and 90–100 kD (not shown). Although the molecular nature of these polypeptides still remains to be shown, this antibody was a useful tool to trace the localization of the GA at the light microscopic level.

Immunofluorescence was performed using 0.5–1-μm sections of unfixed tissue that were quick frozen, freeze dried, and plastic embedded as described elsewhere (14). Primary antibodies were used at IgG concentrations of 10–50 μg/ml. Rhodamine (TRITC)- or fluorescein (FITC)-labeled second antibodies were purchased from Bayer Diagnostic (München, FRG) and Sigma Chemical Co., and were used at dilutions of 1:50 in PBS (pH 7.4). Visualization of two antigens in identical cells was performed by (*a*) immunostaining of adjacent 0.5-μm tissue sections with different antibodies; or (*b*) by simultaneous incubation of the same tissue section with a mixture of two different antibodies raised in two different animal species (e.g., rabbit antivillin and mouse anti-Na^+,K^+-ATPase). The bound primary antibodies were visualized using a mixture of the corresponding secondary antibodies (e.g., swine anti-rabbit IgG, swine anti-mouse IgG) tagged with TRITC and FITC, respectively. The sections were examined with an

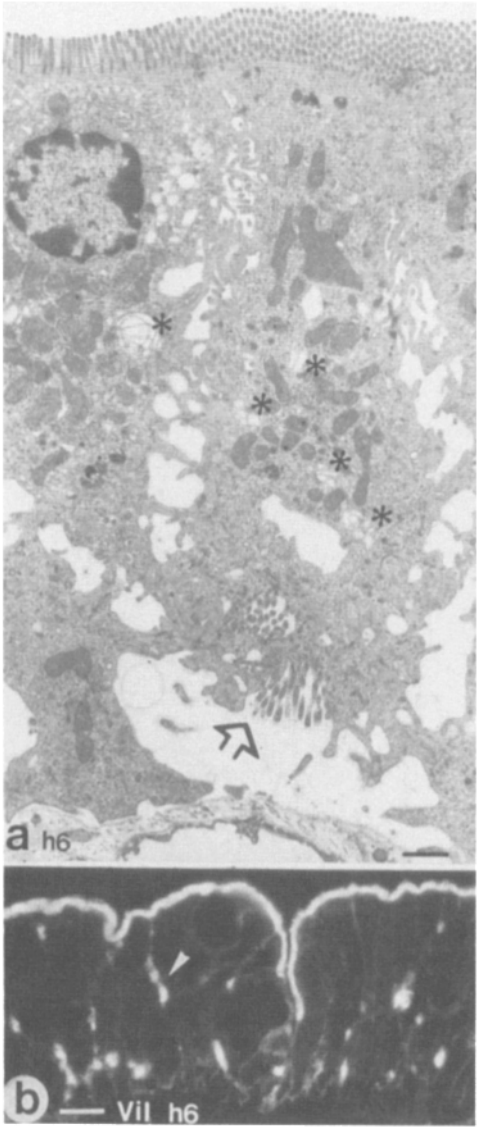

Figure 1. Intestinal epithelium of the mouse 6 h after application of colchicine by stomach tube. (*a*) Electron micrograph showing a basolateral BB located in an invagination of the basal cell surface (*arrow*). Profiles of the dispersed and swollen GA are also seen (*asterisks*). (*b*) Fluorescence micrograph of a corresponding 1-μm-thick section of the epithelium stained with an antibody to villin. Note the numerous basolateral BBs, one of which is indicated by an arrowhead. (*Vil*) Immunostain specific for villin; (*h6*) 6 h after application of colchicine. Bars: (*a*) 1 μm; (*b*) 10 μm.

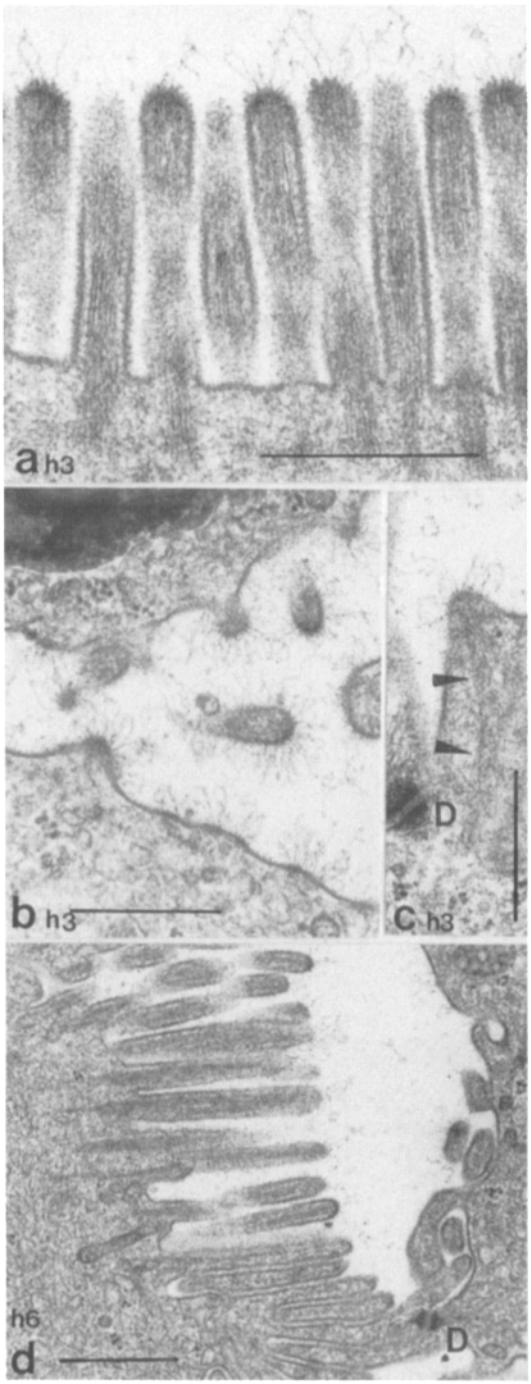

Figure 2. Ultrastructural steps in the formation of basolateral BBs in the rat intestinal epithelium 3 h after application of colchicine. (*a*) Apical BB; note structure of the glycocalyx at the microvillus tip. (*b* and *c*) Area of the basolateral cell surface showing numerous glycocalyx-studded plaques and developing microvilli. Arrowheads point to a microfilament bundle emanating from the cytoplasmic side of a glycocalyx plaque. (*d*) Basolateral BB at 6 h. *D*, desmosome. Bars, 0.5 μm.

Olympus Corp. (New Hyde Park, NY) BH-2 fluorescence microscope equipped with Zeiss objectives and with appropriate filters for TRITC and FITC.

For immunoelectron microscopy, tissue samples were fixed with a mixture of 0.1% glutaraldehyde and 2% paraformaldehyde in PBS (pH 7.4) and embedded in LR White (London Resin Co., Woking, England) as described in detail in a recent study (13, 16). Ultrathin tissue sections were retrieved on gold grids and incubated with primary antibodies and colloidal gold-coupled second antibodies (10 nm), exactly as described elsewhere (13, 16).

Primary antibodies absorbed with their respective antigens served as controls for both immunofluorescence and immunogold labeling.

Results

Formation of Basolateral BBs and BB Vacuoles

As early as 1 h after application of colchicine, individual microvillus-like extensions were observed to emanate from various places along the lateral plasma membrane. At 6 h, the majority of lateral microvilli were locally aggregated at either the basal or lateral membrane surface to form typical BB-like structures (Figs. 1 and 2). Fig. 1 *b* gives an impression of the overall abundance of basolateral BBs. At 12 h, most basolateral BBs had disappeared. Instead, BB-containing vacuoles were observed in the cytoplasm with a preferential occurrence in the infranuclear portion of the cells (Fig. 3). However, BB vacuoles with supranuclear location were also observed at 12 h. As shown by serial sectioning, the BB vacuoles were not continuous with the apical or basolateral cell surface (Fig. 4). The lumens of the BB vacuoles contained numerous free vesicles with a lucent content. These vesicles were probably derived from the shedding of the microvillus membrane as indicated by the presence of a glycocalyx that resembled the glycocalyx of the surrounding microvilli. At 24 and 35 h, the average diameter of the vacuoles had significantly increased in size (from 2–5 μm at 6 h up to 15 μm at 24 h) and the vacuoles were mostly seen in a supranuclear location. BB vacuoles were often seen to fuse with each other and with the apical cell surface (Fig. 4, *d* and *e*).

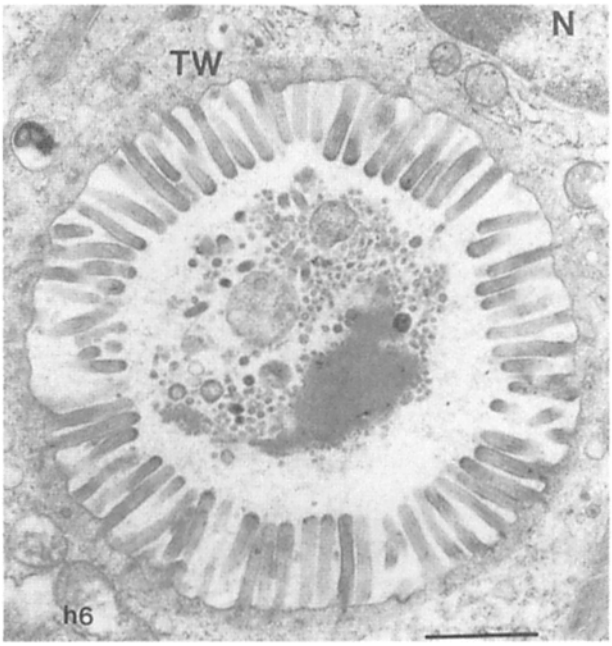

Figure 3. Electron micrograph of a BB vacuole located in the infranuclear cytoplasm of the rat intestinal epithelium 12 h after gavage of colchicine. *N*, nucleus; *TW*, terminal web surrounding the vacuole. Bar, 1 μm.

As shown in Fig. 2 *b*, the initial step of microvillus formation at the basolateral membrane surface was characterized by the occurrence of glycocalyx-studded plaques at the lateral cell surface. These plaques resembled the structure of the glycocalyx associated with the tips of apical microvilli (Fig. 2 *a*). As the microvilli grew, the dense plaques became displaced to the tips of the forming microvilli (Fig. 2, *b* and *c*). The elongation of microvilli was accompanied by the formation of axial core bundles of actin filaments (Fig. 2 *c*). Inhibition of protein synthesis by application of a single dose of cycloheximide at 0 h inhibited the colchicine-induced occurrence of these plaques at the basolateral membrane and the formation of basolateral microvilli. Inhibition of actin polymerization by cytochalasin D (given at 0 and 3 h) did not interfere with the colchicine-induced delivery of glycocalyx-studded plaques to the basolateral surface but inhibited the formation of basolateral microvilli (not shown).

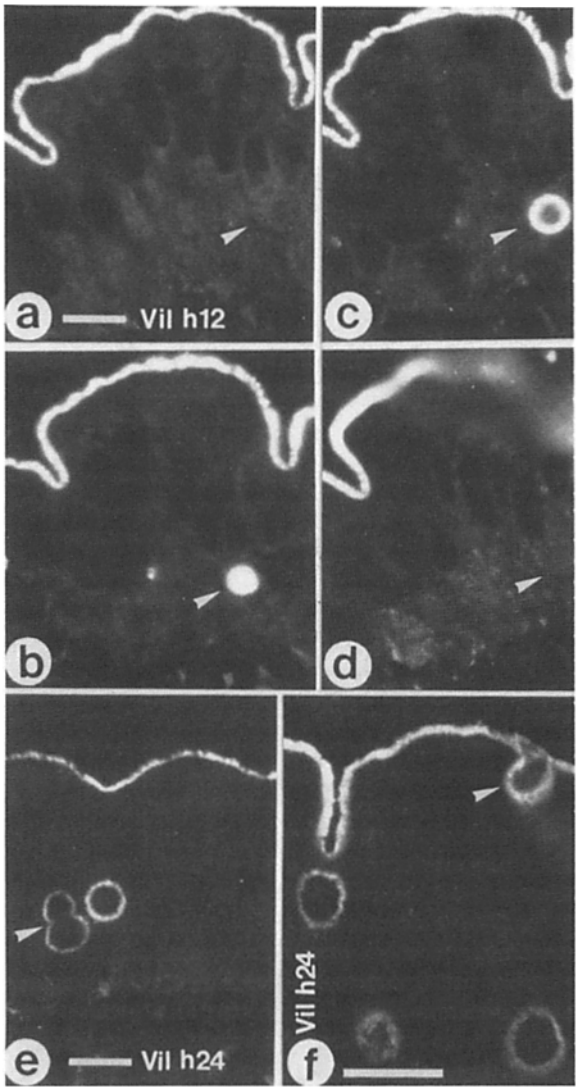

Figure 4. Visualization of BB vacuoles at 12 (*a–d*) and 24 h (*e* and *f*) by antibodies to villin (*Vil*). *a–d* are taken from a series of ten 1-μm-thick sections to show that the BB vacuoles (*arrowheads*) do not represent profiles of invaginations of the apical cell surface. *e* and *f* show fusion of BB vacuoles with each other and with the apical BB (*arrowheads*). Bars, 10 μm.

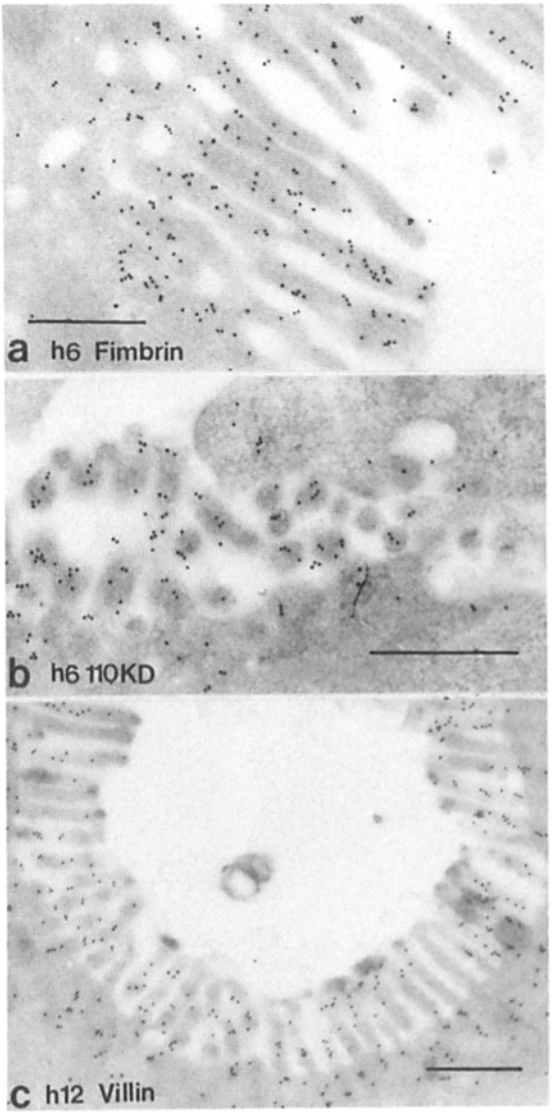

Figure 5. Immunoelectron microscopic localization of fimbrin (*a*), 110-kD protein (*b*), and villin (*c*) in basolateral BBs (*a* and *b*) or a BB vacuole 6 (*a* and *b*) or 12 h (*c*) after application of colchicine. Bars, 0.5 μm.

As described recently, treatment with colchicine (42) and vinblastine (this study) caused considerable reduction in the length of apical microvilli.

The Cytoskeleton of Drug-induced Microvilli

Drug-induced microvilli contained axial core bundles of actin filaments that extended proximally to form a cytoplasmic rootlet (Fig. 2 *d*). The structure of the rootlet area underneath the induced BBs and vacuoles resembled the structure of the terminal web area of the apical BB (Fig. 3). Immunolabeling at the light and electron microscope level demonstrated actin, villin, fimbrin, and the 110-kD protein as regular constituents of the core bundles and rootlets of the induced basolateral microvilli and BB vacuoles (Figs. 1, 4, and 5). The antibody to chicken BB 110-kD protein only cross-reacted with mice but not with rat microvilli.

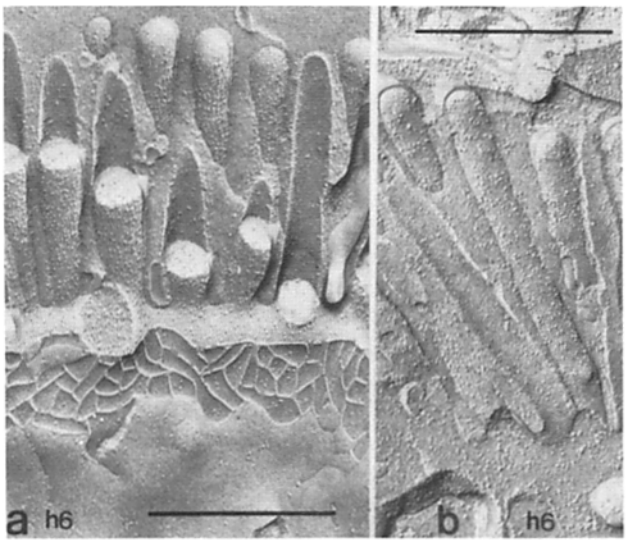

Figure 6. Freeze-fracture image of the rat intestinal epithelium 6 h after gavage of colchicine. In *a*, the apical BB, tight junction, and lateral cell surface is seen. *b* shows part of a basolateral BB. Note differences in the pattern of intramembrane particles between apical and basolateral microvilli as well as between basolateral microvilli and the remaining lateral cell surface. Bars, 0.5 μm.

Freeze-Fracture Studies

Treatment with colchicine did not cause any obvious changes in the structure of the tight junctions examined at 1, 6, and 12 h (Fig. 6 *a*). The density of intramembrane particles associated with both apical and basolateral microvilli was considerably higher than the density of particles present in the remaining (basolateral) cell surface (based on fracture images of 14 basolateral BBs). The P-face of the membrane of the basolateral microvilli (examined at 6 h) differed from that of the apical microvilli, mainly in that the particles were not uniformly distributed within the membrane of the basolateral microvilli but, instead, had a tendency to form clusters (Fig. 6 *b*). These observations indicate differences in the molecular composition between apical and basolateral microvilli. No obvious differences were seen between the E-face of basolateral and apical microvilli. In BB vacuoles (examined at 12 h), the pattern and density of intramembrane particles mostly resembled apical microvilli but BB vacuoles with features of basolateral microvilli were also observed (based on micrographs of nine BB vacuoles).

Microtubules (MTs)

In the intestinal epithelium of untreated mice and rats, antibodies to tubulin revealed a preferential orientation of MTs parallel to the long axis of these columnar epithelial cells (Fig. 7, *a* and *b*). At 30 min, no changes in the MT pattern were seen. At 1 h, MTs had more or less disappeared from the infranuclear portion of the epithelium, whereas MTs were still present in the supranuclear portion (Figs. 7 *c* and 11 *b*). At 6 h, MTs had disappeared from the entire intestinal epithelium except for a narrow zone below the BB (Figs. 7 *d* and 12 *a*). This apical zone (further termed subterminal space) was still brightly labeled with tubulin antibodies but showed a patchy and streaky appearance. At 12 h, numerous MTs had reappeared throughout the cytoplasm (Fig. 7 *e*). The reappearing MTs were less densely packed and less obviously oriented in the cellular long axis. Typically, basket-like formations of MTs were observed around the BB vacuoles (Fig. 7 *e*). At 24 h, the pattern of MTs had reestablished its normal appearance, but basket-like arrays of MTs around the BB vacuoles were still present and persisted over the whole period of observation (up to 35 h). When the reforming MTs were again destroyed by injection of colchicine at 12 h, a patchy and streaky fluorescent band of the antitubulin stain was not only observed underneath the apical BB but also around BB vacuoles (Fig. 8). The same result was obtained when regrowth of MTs was inhibited by a second injection of colchicine at 6 h. 3–6 h later numerous BB vacuoles became visible which were associated with a tubulin-containing rim. Cytoplasmic MTs were largely absent under these conditions.

Golgi Apparatus (GA)

In addition to the induction of basolateral microvilli, treatment with colchicine had a striking effect on the ultrastructure and location of the GA. At 30 min and 1 h, the GA appeared ultrastructurally unchanged (not shown). At 6 h, the GA had disappeared from its normal supranuclear position. Instead, numerous GA-like clusters of smooth vesicles and tubules were observed that were found scattered over the entire sectional profile of the cells (Fig. 1, *asterisks*). These clusters probably represent fragments of the disintegrated GA, as was shown at the light microscope level by immunofluorescence using an antibody reacting with a 55/90-kD GA-associated antigen (Fig. 9). To a certain degree, antibodies to alkaline phosphatase also allowed one to trace the GA by immunofluorescence (Figs. 10 and 11). At 1 h, the supranuclear location and shape of the GA appeared unchanged (Fig. 11 *a*). At 6 and 12 h the GA was completely disrupted, and dotlike fragments of GA-like material were randomly scattered throughout the whole sectional profile of the cell (confirming the electron microscopic observations; Fig. 9, *b* and *c*). At 24 and 35 h, the GA had largely regained its normal shape and supranuclear location (Fig. 9 *d*).

Alkaline Phosphatase

In control animals, antibodies to alkaline phosphatase labeled the BB, the GA in the supranuclear area, as well as numerous cytoplasmic granules located between the GA and the BB (Fig. 10 *b*). At 30 min this pattern appeared unchanged. At 1 h, the immunolabeling also became visible along the basolateral membrane surface, whereas the GA-like immunofluorescence still appeared normal (Fig. 11 *a*). At 6 h, the intensity of the immunofluorescence associated with the basolateral cell surface had further increased (Fig. 10 *d*). The intensity of immunofluorescence overlying the colchicine-induced basolateral BBs did not significantly differ from the staining intensity of the remaining basolateral cell surface. The GA was no longer visible. Instead, numerous fluorescent dots crowded the cytoplasm from the base toward the apex (Fig. 10 *d*). At 12 h, the immunolabeling associated with the basolateral cell surface had largely disappeared. Strong immunolabeling was then observed overlying the microvilli of virtually all BB vacuoles (Fig. 10 *f*). The contents of the BB vacuoles were also brightly labeled. Delivery of alkaline phosphatase to the BB vacuoles did not de-

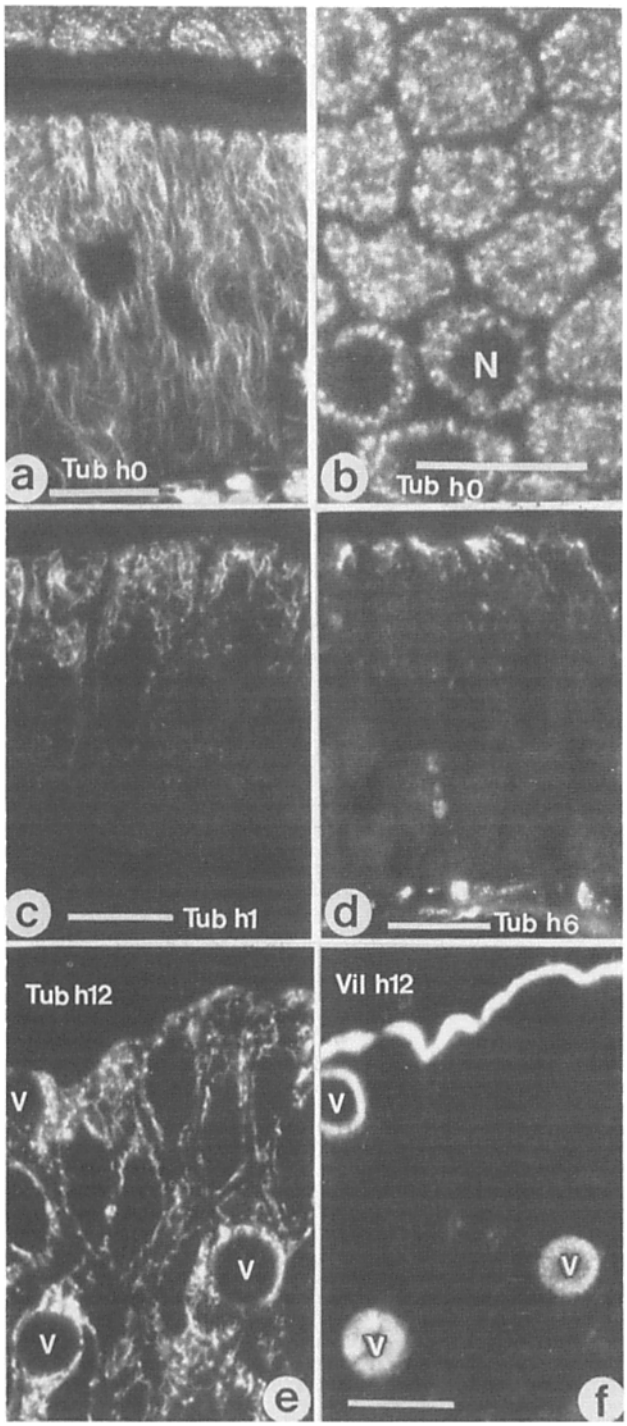

Figure 7. Immunofluorescence pattern of MTs (*Tub*) in the intestinal epithelium of control rats (*a* and *b*) and rats treated with colchicine and killed at 1 (*c*), 6 (*d*), and 12 h (*e*) after drug application by stomach tube. *b* is a high magnification view of a cross-section of the epithelium at the nuclear (*N*) and supranuclear level. *e* and *f* are adjacent 0.5-μm sections stained with antitubulin (*Tub*) (*e*) and antivillin (*Vil*) (*f*). Note preferential association of MTs around BB vacuoles (*V*). Bars, 10 μm.

pend on the presence of MTs because immunostaining of the BB vacuoles was not significantly reduced in rats that had received a second dose of colchicine at 6 h or were treated with a single dose of vinblastine at 0 h. Administration of 15 mg/kg vinblastine largely inhibited reassembly of MTs within a period of 12 h, but did not interfere with the formation of BB vacuoles (Fig. 14). At 24 and 35 h, the pattern of immunofluorescence resembled controls except for the presence of strongly labeled BB vacuoles that were still present in large numbers at 35 h (not shown). Application of cycloheximide completely inhibited the colchicine-induced delivery of alkaline phosphatase to the GA and the basolateral cell surface (Fig. 12 *b*). Gavage of cycloheximide at 6 and 9 h did not inhibit formation of BB vacuoles and assembly of their cytoskeleton, but inhibited delivery of alkaline phosphatase to the BB vacuoles that were examined by immunofluorescence 3–6 h later (at 12 h) (Fig. 12 *d*).

Sucrase-Isomaltase and Aminopeptidase N

Antibodies to sucrase-isomaltase and aminopeptidase N gave basically the same results as were described in detail for antibodies against alkaline phosphatase. Both antibodies reacted strongly with intestinal epithelium of mice but rather weakly with that of rats. The GA was only faintly labeled with these antibodies. After treatment with colchicine, there was a slight increase in the immunostain along the lateral plasma membrane. At 12 h all BB vacuoles including their vesicular contents were brightly labeled with both antibodies (Fig. 13).

Na^+,K^+-ATPase

Antibodies to kidney Na^+,K^+-ATPase reacted selectively with the lateral cell surface of the intestinal epithelium. No changes of the staining pattern were seen after treatment with colchicine or vinblastine (Fig. 14 *a*). Simultaneous visualization of basolateral BBs, BB vacuoles (by antibodies to villin), and Na^+,K^+-ATPase revealed that the Na^+,K^+-ATPase was absent from those sites of the basolateral plasma membrane that were occupied by BBs. There was also no immunolabeling for Na^+,K^+-ATPase in association with the BB vacuoles (Fig. 14 *a*). Experiments with rats treated with cycloheximide showed considerable reduction and local disappearance of the immunolabeling within a period of 12 h after gavage of a single dose (14 mg/kg body weight). This indicates a rather high turnover of the Na^+,K^+-ATPase under these conditions.

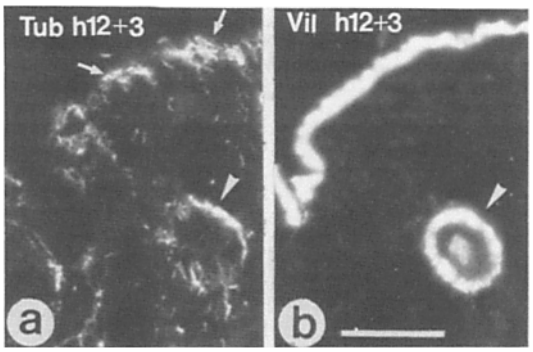

Figure 8. Depolymerization of MTs by a second application of colchicine at 12 h. The rats were killed 3 h later (*h 12 +3*). Serial sections of the epithelium were processed for immunostaining with antitubulin (*Tub*) (*a*) and antivillin (*Vil*) (*b*). Note concentration of MTs underneath the apical BB (*arrows*) and around BB vacuoles (*arrowhead*). Bar, 10 μm.

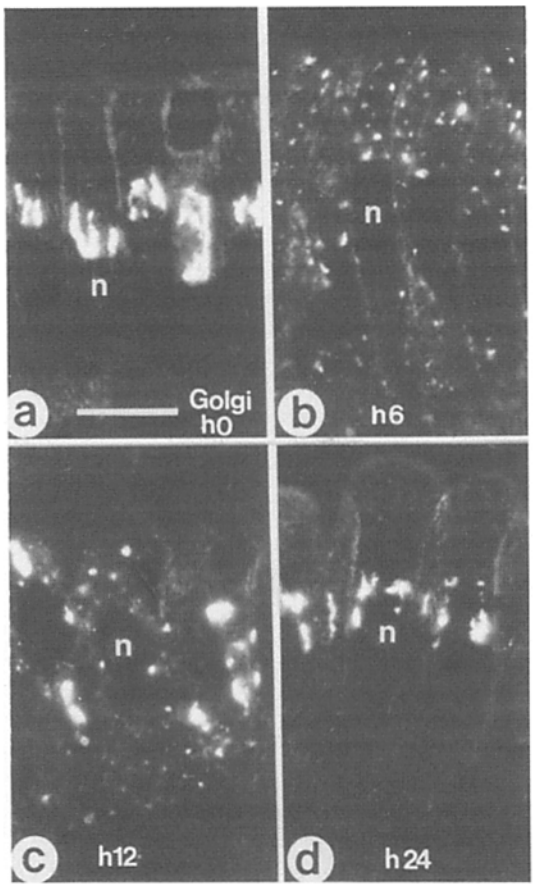

Figure 9. Localization of the GA by immunofluorescence (using a 55-kD Golgi-specific antibody) in the intestinal epithelium of rats treated with colchicine and killed immediately (*h0*) (*a*), or 6 (*b*), 12 (*c*), or 24 h (*d*) after application of the drug. Positions of cell nuclei (*n*) are indicated. Bar, 10 μm.

Discussion

Role of MTs in Polarized Delivery of Apical Membrane Proteins

In the present study on the rat and mouse intestinal epithelium, we have used an immunocytochemical approach to study the role of MTs in generation and maintenance of cell polarity. In confirmation and extension of previously published studies (see Introduction), we show that depolymerization of MTs by colchicine and vinblastine selectively interferes with the polarized delivery of membrane proteins destined for the apical plasma membrane; whereas correct targeting of Na^+,K^+-ATPase, a basolaterally located membrane protein, appeared unaffected.

The occurrence of apical membrane proteins at the basolateral cell surface was not caused by a possible disturbance of the structure of tight junctions. Our freeze-fracture studies and recent peroxidase tracer studies (18) did not reveal any detectable effect of colchicine on the structure and tightness of tight junctions in the rat intestinal epithelium. These findings are consistent with a study reporting that nocodazole and colchicine have no significant effect on transepithelial resistance in Madin–Darby canine kidney (MDCK) cells (35). Inhibition of protein synthesis by cycloheximide suppressed completely the occurrence of apical enzymes and BBs at the basolateral domain of colchicine-treated animals. The latter experiment shows that changes in cell polarity were not caused by redistribution (displacement) of preexisting apical membrane proteins to the basolateral domain but, rather, resulted from delivery of significant amounts of newly synthesized proteins to the wrong (basolateral) membrane domain. Mistargeting of apical membrane proteins is probably

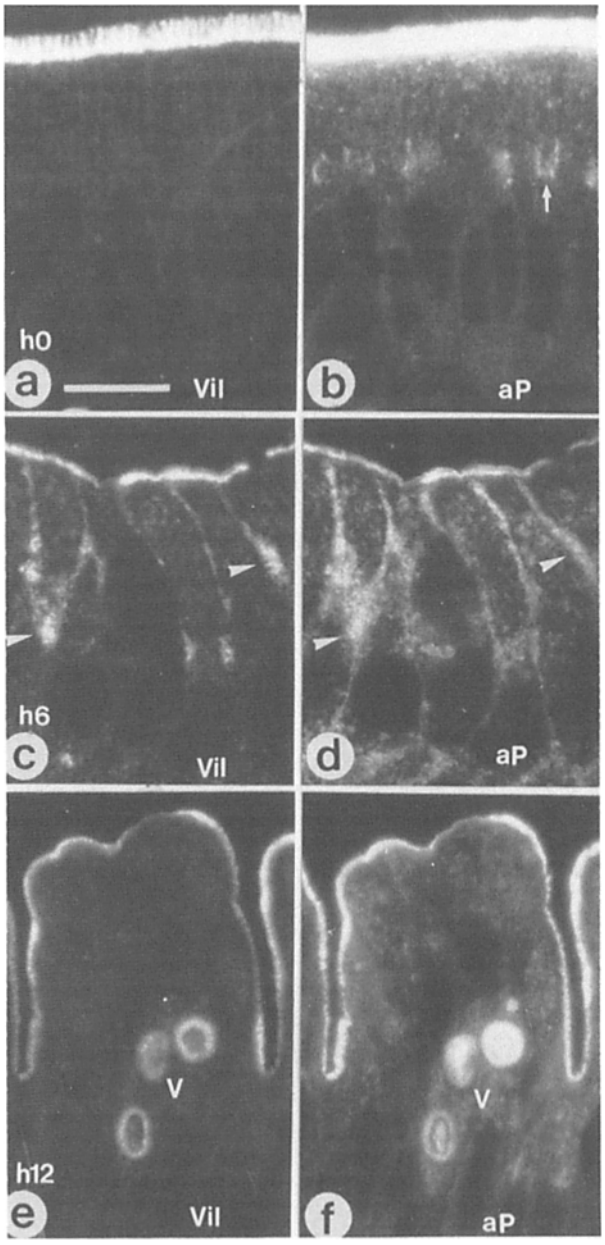

Figure 10. Simultaneous localization of villin (*Vil*) (*a*, *c*, and *e*) and alkaline phosphatase (*aP*) (*b*, *d*, and *f*) in the intestinal epithelium of control rats (*h0*) (*a* and *b*) and rats treated with colchicine and killed 6 (*c* and *d*) and 12 h (*e* and *f*) later. Note alkaline phosphatase stain along the entire basolateral cell surface at 6 h (*d*) and within BB vacuoles (*V*) at 12 h (*f*). Arrowheads in *c* point to basolateral BBs. In controls (*b*) the GA (*arrow*) is also seen. Fluorescent particles located between the GA and the BB probably represent apical CVs. Bar, 10 μm.

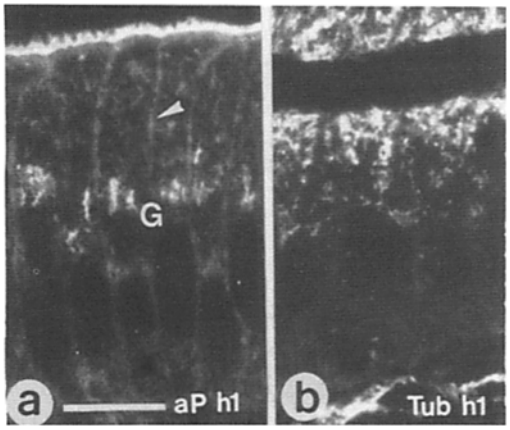

Figure 11. Occurrence of alkaline phosphatase (*aP*) at the basolateral cell surface (*arrowhead*) 1 h after application of colchicine (*a*). The location of the GA (*G*) appears normal (compare with Figs. 9 *a* and 10 *b*), whereas the pattern of MTs (*Tub*) stained in *b* has already considerably changed (compare with Fig. 7 *a*). Bar, 10 μm.

also not a result of fragmentation and dispersal of the GA that has been shown in this and a previous study (41) to accompany depolymerization of MTs. Delivery of apical enzymes to the basolateral cell surface and formation of basolateral microvilli became already visible at 1 h after gavage of colchicine, when MTs were partially or completely destroyed but the GA was still located in its normal supranuclear position (Fig. 11). On the other hand, the disappearance of apical enzymes from the basolateral cell surface between 6 and 12 h (Fig. 10 *f*) correlated precisely with the reappearance of MTs (Fig. 7 *e*). At this stage, the GA was still heavily fragmented and dispersed throughout the cell (Fig. 9 *c*). Thus, polarized targeting of apical membrane proteins was closely related to the integrity of the MT system and did not depend on the supranuclear position and morphological integrity of the GA.

These findings largely support observations on the effect of depolymerization of MTs on the apical budding of influenza virus in MDCK cells (47). Disruption of MTs by colchicine and nocodazole caused random budding of influenza virus (for contradictory results see reference 49), whereas basolateral budding of stomatitis virus appeared unaffected by these drugs. The most likely explanation for these observations is that apically destined "carrier vesicles" (CVs) (36) contain a receptor for MTs or MT-associated proteins that are responsible for MT-dependent transport to the apical plasma membrane. The transport mechanism for apical CVs may be similar to the mechanism underlying the fast axonal transport which is mediated by MTs and MT-associated proteins (54). As shown by fluorescence microscopy in this study and by a previously published immunoelectron microscope study (13), MTs of the intestinal epithelium are preferentially aligned in an apicobasal orientation (Fig. 7, *a* and *b*). This particular alignment of MTs may guarantee that apical CVs leaving the GA will be vectorially guided to the apical surface. As soon as MTs become depolymerized by colchicine or vinblastine, the apical CVs lose their "tracks" and thus diffuse randomly throughout the cell. A fraction of the vesicles (40–60% according to [^{3}H]fucose autoradiography quantified in references 3, 4, and 19) may still happen to reach the apical membrane whereas others fuse with the basolateral membrane and thus deliver apically destined proteins (such as the BB enzymes or the glycocalyx-studded plaque proteins of the microvillus tip) to the basolateral cell surface (~50% according to [^{3}H]fucose autoradiography, reference 19).

This model demands that basolateral CVs do not contain any signal for transport along MTs and therefore follow the bulk flow of membranes that appears to be directed to the basolateral membrane domain in the intestinal epithelium (48). However, as will be discussed later, there must be an additional mechanism that prevents basolateral CVs from fusing with the apical membrane.

Role of the Apical Subterminal Space in MT Organization

The cytoplasmic space located adjacent to the apical terminal web of the intestinal epithelium has been shown to contain the centrosome, which is absent from the area of the GA (13, 50). As demonstrated in this study, the subterminal space appears to be the major site for organization of MT growth. After application of colchicine, depolymerization of microtubules proceeded continuously in a basal to apical direction.

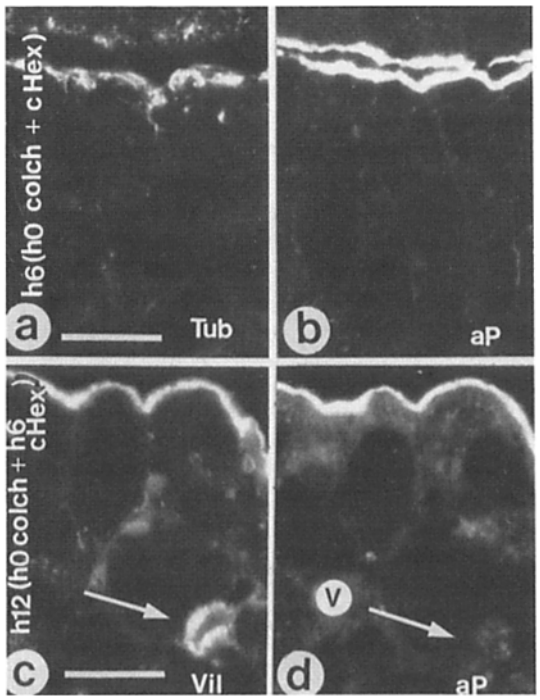

Figure 12. Intestinal epithelium of rats treated either simultaneously with colchicine and cycloheximide (*h0 colch + cHex*) (*a* and *b*) or first with colchicine and 6 h later with cycloheximide (*h0 colch + h6 cHex*) (*c* and *d*). Animals were killed 6 (*a* and *b*) and 12 h (*c* and *d*) after gavage of colchicine, respectively, and processed for immunostaining with antibodies to alkaline phosphatase (*aP*) (*b* and *d*), tubulin (*Tub*) (*a*), or villin (*Vil*) (*c*). Cycloheximide inhibited occurrence of alkaline phosphatase in the GA and at both the basolateral surface and the BB vacuoles (*arrows*, *V*). Cycloheximide did not interfere with colchicine-induced depolymerization of MTs and delivery of cytoskeletal proteins to the BB vacuoles (*c*). Bars, 10 μm.

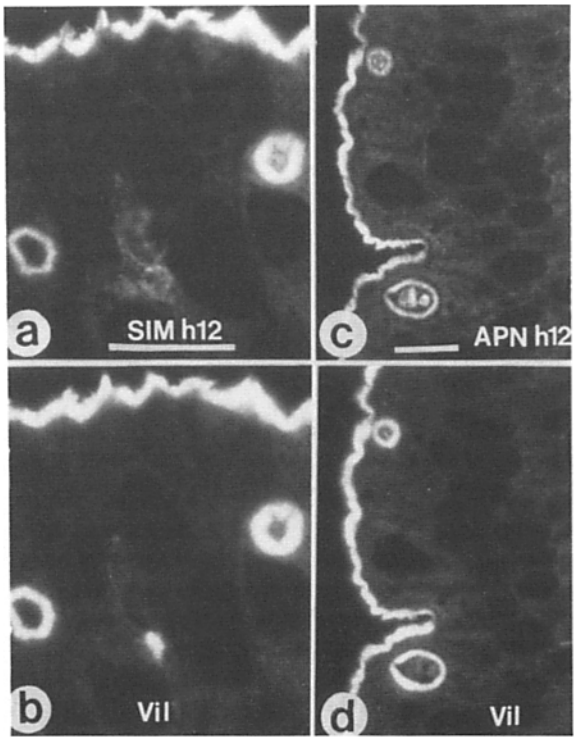

Figure 13. Association of sucrase–isomaltase (*SIM*) (*a*) and aminopeptidase N (*APN*) (*c*) with colchicine-induced BB vacuoles in the intestinal epithelium of mice killed at 12 h. Simultaneous localization of BB vacuoles by villin (*Vil*) is shown in *b* and *d*. Bars, 10 μm.

Typically, at 1 h MTs had disappeared from the infranuclear space but were still present in the apical half or third of the epithelial cells (Figs. 7 *c* and 11 *b*). At 3 h all MTs were depolymerized except for a few microtubules confined to the subterminal space. This space is also the preferential site for vinblastine-induced paracrystals of tubulin (not shown). Regrowth of MTs always proceeded from the subterminal space in a basal direction. The MT-stabilizing and -organizing property of the subterminal space appears not to be associated with the centrosome because MT-organizing properties were also located in the periphery of the BB vacuoles, where no centrosomes were detected. The MT-organizing activity of the subterminal space may be important for the polarized organization of the MT system and thus for the polarized transport of apical membrane proteins. Since the slowly growing end of MTs must be located in the subterminal space, we suggest that apical CVs are targeted to the BB by a retrograde transport mechanism. Recently, the microtubule-associated protein MAP IC has been identified as a potential candidate for such a retrograde motor of cytoplasmic MTs (55).

In hepatocytes, which are multipolarized epithelial cells, MTs are not aligned to the rather small apical-like domain of the bile canaliculi (unpublished observations). Thus, it is not surprising that in hepatocytes the bulk of membrane proteins is delivered to the predominating membrane surface of the cells, which is the sinusoidal and lateral domain. By a still unknown secondary mechanism, the apical proteins become subsequently redistributed to the canalicular (apical) membrane whereas the basolateral proteins remain in the lateral and sinusoidal membrane (2). Whether a similar two-step mechanism may also operate in the apical delivery of certain membrane proteins in the intestinal epithelium is still a matter of dispute (1, 25, 43).

Reconstitution of Cell Polarity and the Role of BB Vacuoles

Reconstitution of cell polarity occurred in three steps: (*a*) displacement of basolateral BBs into invaginations, (*b*) internalization of the BBs to form BB vacuoles, and (*c*) fusion of BB vacuoles with the apical BB. Apical fusion was often preceded by fusion of BB vacuoles with each other. Since fusion of BB vacuoles with the apical cell surface has not been observed at the ultrastructural level, we cannot exclude the possibility that the primary site of fusion is located at the lateral cell surface close to the tight junctions as described recently for the fusion of microvillus-studded vacuoles in MDCK cells at low Ca^{2+} (57). By subsequent opening of the tight junctions, the vacuolar membrane could be incorporated into the apical membrane domain (57).

BB vacuoles resembled the apical BB with respect to ultrastructure, composition of the cytoskeleton, presence of high concentration of BB enzymes and MT-organizing properties (see above). As shown by the experiments performed with cycloheximide, only newly synthesized BB enzymes were delivered to the BB vacuoles. This suggests that CVs containing apical membrane proteins are released from the dispersed GA at any place within the cell. MTs probably serve as guidelines that target the apical CVs to either the BB vacuoles or the apical BB. In the absence of MTs, the apical CVs will randomly diffuse within the cell and by chance fuse with the BB vacuoles, the apical, or basolateral membranes. This interpretation is based on the observation that in the presence of MTs (which regrow between 6 and 12 h) the apical enzymes were concentrated within the BB vacuoles and the apical BB but were largely absent from the basolateral membrane. In the absence of MTs (reinjection of colchicine, single dose of vinblastine), the BB enzymes were also present at the basolateral cell surface (not shown).

Microvillus-studded vacuoles have also been observed in tumors and tumor cell lines derived from various kinds of polarized epithelial cells (31, 44, 53). In certain cases of pan-

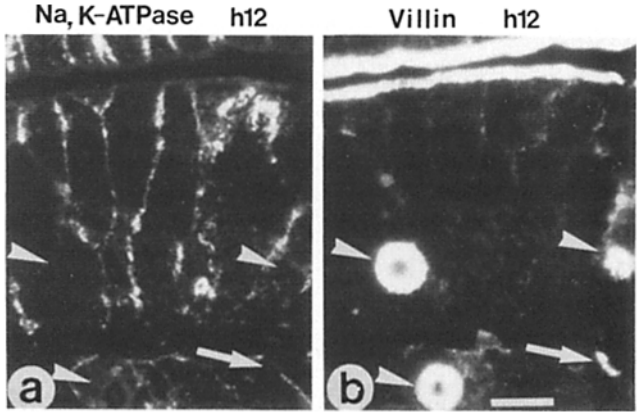

Figure 14. Simultaneous visualization of Na^+,K^+-ATPase (*a*) and villin (*b*) in the intestinal epithelium of rats treated with vinblastine and killed 12 h later. Note absence of Na^+,K^+-ATPase stain from the apical BB, BB vacuoles (*arrowheads*), and basolateral BBs (*arrow*). Bar, 10 μm.

creatic carcinoma both BB vacuoles and basolateral microvilli have been observed in the same cell (29). BB vacuoles also occur in the fetal intestine (10) and in thyroid cells (45) where these vacuoles appear to play a key role in lumen formation and morphogenesis. In the light of the present experiments and in view of recently published experiments obtained with MDCK cells (56, 57), formation of BB vacuoles may be considered as a part of the mechanism by which epithelial cells regain polarity.

Exclusion of Na^+,K^+-ATPase from Basolateral BBs and BB Vacuoles

Our experiments with cycloheximide indicate a rather high turnover of the Na^+,K^+-ATPase. Immunostain specific for Na^+,K^+-ATPase was confined to the basolateral cell surface but was clearly excluded from those sites of the basolateral domain that were occupied by the drug-induced basolateral BBs (Fig. 14). On the other hand, the mistargeted apical enzymes were evenly distributed along the entire basolateral cell surface including the basolateral BBs. Since the freeze-fracture studies showed that the basolateral BBs were not sealed from the remaining basolateral cell surface by tight junctions, we suggest that the Na^+,K^+-ATPase cannot freely diffuse within the plane of the lipid bilayer. This view is further supported by recent studies showing that Na^+,K^+-ATPase has a binding site for ankyrin which may function to tether the Na^+,K^+-ATPase to the spectrin-based membrane cytoskeleton (30, 39). A similar mechanism is probably involved in placing the kidney band 3–like anion exchanger at specialized microdomains of the basolateral membrane surface of the collecting duct epithelium (17).

Na^+,K^+-ATPase was not delivered to the BB vacuoles. This is surprising since the probability of Na^+,K^+-ATPase–containing CVs to fuse with BB vacuoles should be as high as the probability of apical CVs to fuse with BB vacuoles in the absence of MTs. These observations indicate that basolateral CVs might not be able to fuse with the membrane of BB vacuoles. In support of these observations, recent experiments with MDCK cells have shown that influenza virus hemagglutinin, an apically targeted glycoprotein, is concentrated within microvillus-studded vacuoles, whereas the basolateral glycoprotein G of vesicular stomatitis virus is excluded from these vacuoles (56).

A Hypothesis for Polarized Targeting of Membrane Proteins (Transport Barrier Hypothesis)

A central conclusion drawn from the present experiments and experiments with virus-infected MDCK cells (47) is that apical CVs can fuse with both the apical and basolateral plasma membrane, whereas basolateral CVs seem to be only able to fuse with the basolateral and not the apical membrane domain. Most likely, apical CVs are largely prevented from fusion with the basolateral domain by selective transport along MTs to the apical cell pole. Delivery of basolateral CVs to the basolateral cell surface probably does not depend on MTs, but rather appears to follow the bulk flow of membranes which is directed to the basolateral surface in the intestinal epithelium (48). At present it is not known why basolateral CVs do not fuse with the apical cell surface or with BB vacuoles. One major structural difference between the apical and basolateral membrane domain is the elaborate cytoskeleton of the terminal web that underlies the plasma membrane of the BB and the BB vacuoles (7, 13, 38). Such an elaborate web is absent from the basolateral membrane. Since MTs only rarely project into the terminal web (14, 24, 50), the bulk of apical CVs must be able to move through this filamentous meshwork by a mechanism that is independent of MTs. Recent immunoelectron microscopic observations indicate association of vesicles in the terminal web with the 110-kD protein (13). The 110-kD protein is a myosin-related mechanoprotein (8, 9) which is probably able to cause movements of vesicles along actin filaments (8). It is tempting to speculate that the 110-kD protein or some other component of the terminal web binds only to the apical CVs and thus might facilitate selective access of apical CVs to the apical lipid bilayer, whereas basolateral CVs might be excluded by such a mechanism.

This work was supported by the Deutsche Forschunggemeinshaft (Kl 238/1-1, 8).

Received for publication 27 December 1988 and in revised form 6 March 1989.

References

1. Ahnen, D. J., N. A. Santiago, J.-P. Cezard, and G. M. Gray. 1982. Intestinal amino-oligopeptidase. In vivo synthesis on intracellular membranes of rat jejunum. *J. Biol. Chem.* 257:12129–12135.
2. Bartels, J. R., H. M. Feracci, B. Stieger, and A. L. Hubbard. 1987. Biogenesis of the rat hepatocyte plasma membrane in vivo: comparison of the pathways taken by apical and basolateral proteins using subcellular fractionation. *J. Cell Biol.* 105:1241–1251.
3. Bennett, G., E. Carlet, G. Wild, and S. Parsons. 1984. Influence of colchicine and vinblastine on the intracellular migration of secretory and membrane glycoproteins. *III.* Inhibition of intracellular migration of membrane glycoproteins in rat intestinal columnar cells and hepatocytes as visualized by light and electron microscope radioautography after ^{3}H-fucose injection. *Am. J. Anat.* 170:545–566.
4. Blok, J., L. A. Ginsel, A. A. Molder-Stapel, J. J. M. Onderwater, and W. T. Daems. 1981. The effect of colchicine on the intracellular transport of ^{3}H-fucose-labelled glycoproteins in the absorptive cells of cultured human small-intestinal tissue. An autoradiographical and biochemical study. *Cell Tissue Res.* 215:1–12.
5. Brunser, O., and J. H. Luft. 1970. Fine structure of the apex of absorptive cells from rat small intestine. *J. Ultrastruct. Res.* 31:291–311.
6. Buchheim, W., D. Drenckhahn, and R. Lüllmann-Rauch. 1979. Freeze-fracture studies of cytoplasmic inclusions occurring in experimental lipidosis as induced by amphiphilic cationic drugs. *Biochim. Biophys. Acta.* 575:71–80.
7. Burgess, D. R. 1987. The brush border: a model for structure, biochemistry, motility and assembly of the cytoskeleton. *Adv. Cell Biol.* 1:31–58.
8. Carboni, J. M., K. A. Conzelman, R. A. Adams, D. A. Kaiser, T. D. Pollard, and M. S. Mooseker. 1988. Structural and immunological characterization of the myosin-like 110-kD subunit of the intestinal microvillar 110K-calmodulin complex: evidence for discrete myosin head and calmodulin-binding domain. *J. Cell Biol.* 107:1749–1757.
9. Collins, J. H., and C. W. Borysenko. 1984. The 110,000-dalton actin- and calmodulin-binding protein from intestinal brush border is a myosin-like ATPase. *J. Biol. Chem.* 259:14128–14135.
10. Colony, P. C., and M. R. Neutra. 1983. Epithelial differentiation in the fetal rat colon. I. Plasma membrane phosphatase activities. *Dev. Biol.* 97:349–363.
11. Danielsen, E. M., and G. M. Cowell. 1985. Biosynthesis of intestinal microvillar proteins: evidence for an intracellular sorting taking place in, or shortly after, exit from the Golgi complex. *Eur. J. Biochem.* 152: 493–499.
12. Danielsen, E. M., G. M. Cowell, and S. S. Poulsen. 1983. Biosynthesis of intestinal microvillar proteins: role of Golgi complex and microtubules. *Biochem. J.* 216:37–42.
13. Drenckhahn, D., and R. Dermietzel. 1988. Organization of the actin-filament cytoskeleton in the intestinal brush border: a quantitative and qualitative immunoelectron microscope study. *J. Cell Biol.* 107:1037–1048.
14. Drenckhahn, D., and H. Franz. 1986. Identification of actin, alpha-actinin, and vinculin-containing plaques at the lateral membrane of epithelial cells. *J. Cell Biol.* 102:1843–1852.
15. Drenckhahn, D., and U. Gröschel-Stewart. 1980. Localization of myosin,

actin, and tropomyosin in rat intestinal epithelium: immunohistochemical studies at the light and electron microscope levels. *J. Cell Biol.* 86:475-482.
16. Drenckhahn, D., and C. Merte. 1987. Restriction of the human kidney band 3-like anion exchanger to specialized subdomains of the basolateral plasma membrane of intercalated cells. *Eur. J. Cell Biol.* 45:107-115.
17. Drenckhahn, D., K. Schlüter, D. P. Allen, and V. Bennett. 1985. Colocalization of band 3 with ankyrin and spectrin at the basal membrane of intercalated cells in the rat kidney. *Science (Wash. DC).* 230:1287-1289.
18. Ellinger, A., and M. Pavelka. 1986. Colchicine-induced tubular, vesicular and cisternal organelle aggregates in absorptive cells of the small intestine of the rat. II. Endocytosis studies. *Biol. Cell.* 58:31-42.
19. Ellinger, A., M. Pavelka, and A. Gangl. 1983. Effect of colchicine on rat small intestinal absorptive cells. II. Distribution of label after incorporation of (^{3}H)fucose into plasma membrane glycoproteins. *J. Ultrastruct. Res.* 85:260-271.
20. Feracci, H., and S. Maroux. 1980. Rabbit intestinal aminopeptidase N. Purification and molecular properties. *Biochim. Biophys. Acta.* 599:448-463.
21. Fujita, M., H. Ohta, K. Kawai, H. Matsui, and M. Nakao. 1972. Differential isolation of microvillous and basolateral plasma membranes from intestinal mucosa: mutually exclusive distribution of digestive enzymes and ouabain-sensitive ATPase. *Biochim. Biophys. Acta.* 274:336-347.
22. Ghersa, P., P. Huber, G. Semenza, and H. Wacker. 1986. Cell-free synthesis, membrane integration, and glycosylation of pro-sucrase-isomaltase. *J. Biol. Chem.* 261:7969-7974.
23. Griffiths, G., and K. Simons. 1986. The *trans* Golgi network: sorting at the exit site of the Golgi complex. *Science (Wash. DC).* 234:438-443.
24. Hagen, S. J., C. H. Allan, and J. S. Trier. 1987. Demonstration of microtubules in the terminal web of mature absorptive cells from the small intestine of the rat. *Cell Tissue Res.* 248:709-712.
25. Hauri, H.-P., A. Quaroni, and K. J. Isselbacher. 1979. Biosynthesis of intestinal plasma membrane: posttranslational route and cleavage of sucrase-isomaltase. *Proc. Natl. Acad. Sci. USA.* 76:5183-5186.
26. Hauri, H.-P., E. E. Sterchi, D. Bienz, J. A. M. Fransen, and A. Marxen. 1985. Expression and intracellular transport of microvillus membrane hydrolases in human intestinal epithelial cells. *J. Cell Biol.* 101:838-851.
27. Hugon, J. S., G. Bennett, P. Pothier, and Z. Ngoma. 1987. Loss of microtubules and alteration of glycoprotein migration in organ cultures of mouse intestine exposed to nocodazole or colchicine. *Cell Tissue Res.* 248:653-662.
28. Kenny, J., and A. J. Turner. 1987. Mammalian Ectoenzymes. Elsevier Science Publishing Co., New York. 360 pp.
29. Kern, H. F., H. D. Röher, M. von Bülow, and G. Klöppel. 1987. Fine structure of three major grades of malignancy of human pancreatic adenocarcinoma. *Pancreas.* 2:2-13.
30. Koob, R., M. Zimmermann, W. Schoner, and D. Drenckhahn. 1987. Colocalization and coprecipitation of ankyrin and Na^+,K^+-ATPase in kidney epithelial cells. *Eur. J. Cell Biol.* 45:230-237.
31. Le Bivic, A., M. Hirn, and H. Reggio. 1988. HT-29 cells are an in vitro model for the generation of cell polarity in epithelia during embryonic differentiation. *Proc. Natl. Acad. Sci. USA.* 85:136-140.
32. Madara, J. L., and J. S. Trier. 1986. Functional morphology of the mucosa of the small intestine. *In* Physiology of the Gastrointestinal Tract. 2nd edition. L. R. Johnson, editor. Raven Press, New York. 44 pp.
33. Matlin, K. S., and K. Simons. 1984. Sorting of a plasma membrane glycoprotein occurs before it reaches the cell surface in cultured epithelial cells. *J. Cell Biol.* 99:2131-2139.
34. Matsudaira, P. T., and D. R. Burgess. 1982. Organization of the cross-filaments in intestinal microvilli. *J. Cell Biol.* 92:657-664.
35. Meza, I., G. Ibarra, M. Sabanero, A. Martinez-Palomo, and M. Cereijido. 1980. Occluding junctions and cytoskeletal components in a cultured transporting epithelium. *J. Cell Biol.* 87:746-754.
36. Michaels, J. E., and C. P. Leblond. 1976. Transport of glycoprotein from Golgi apparatus to cell surface by means of "carrier vesicles", as shown by radioautography of mouse colonic epithelium after injection of ^{3}H-fucose. *J. Microsc. Biol. Cell.* 25:243-248.
37. Misek, D. E., E. Bard, and E. J. Rodriguez-Boulan. 1984. Biogenesis of epithelial cell polarity: intracellular sorting and vectorial exocytosis of an apical plasma membrane glycoprotein. *Cell.* 39:537-546.
38. Mooseker, M. S. 1985. Organization, chemistry, and assembly of the cytoskeletal apparatus of the intestinal brush border. *Annu. Rev. Cell Biol.* 1:209-241.
39. Nelson, W. J., and P. J. Veshnock. 1987. Ankyrin binding to (Na^+ + K^+) ATPase and implications for the organization of membrane domains in polarized cells. *Nature (Lond.).* 328:533-536.
40. Neutra, M. R. 1988. The gastrointestinal tract. *In* Cell and Tissue Biology. L. Weiss, editor. Urban & Schwarzenberg, Baltimore, MD. 643-683.
41. Pavelka, M., and A. Ellinger. 1981. Effect of colchicine on the Golgi apparatus and on GERL of rat jejunal absorptive cells. Ultrastructural localization of thiamine pyrophosphatase and acid phosphatase activity. *Eur. J. Cell Biol.* 24:53-61.
42. Pavelka, M., A. Ellinger, and A. Gangl. 1983. Effects of colchicine on rat small intestinal absorptive cells. I. Formation of basolateral microvillus borders. *J. Ultrastruct. Res.* 85:249-259.
43. Quaroni, A., K. Kirsch, and M. M. Weiser. 1979. Synthesis of membrane glycoproteins in rat small-intestinal villus cells: effect of colchicine on the redistribution of L-(1,5,6-^{3}H)fucose-labelled membrane glycoproteins among Golgi, lateral, basal and microvillus membranes. *Biochem. J.* 182:213-221.
44. Remy, L. 1986. The intracellular lumen: origin, role, and implications of a cytoplasmic neostructure. *Biol. Cell.* 56:97-106.
45. Remy, L., M. Michel-Bechet, C. Cataldo, J. Bottini, S. Hovsepian, and G. Fayet. 1977. The role of intracellular lumina in thyroid cells for follicle morphogenesis in vitro. *J. Ultrastruct. Res.* 61:243-253.
46. Rindler, M. J., I. E. Ivanov, H. Plesken, and D. D. Sabatini. 1985. Polarized delivery of viral glycoproteins to the apical and basolateral plasma membranes of MDCK cells infected with temperature-sensitive viruses. *J. Cell Biol.* 100:136-151.
47. Rindler, M. J., I. E. Ivanov, and D. D. Sabatini. 1987. Microtubule-acting drugs lead to the nonpolarized delivery of the influenza hemagglutinin to the cell surface of polarized Madin-Darby canine kidney cells. *J. Cell Biol.* 104:231-241.
48. Rindler, M. J., and M. G. Traber. 1988. A specific sorting signal is not required for the polarized secretion of newly synthesized proteins from cultured intestinal epithelial cells. *J. Cell Biol.* 107:471-479.
49. Salas, P. J. I., D. E. Misek, D. E. Vega-Salas, D. Gundersen, M. Cereijido, and E. Rodriguez-Boulan. 1986. *Microtubules* and actin filaments are not critically involved in the biogenesis of epithelial cell surface polarity. *J. Cell Biol.* 102:1853-1867.
50. Sandoz, D., M.-C. Laine, and G. Nicholas. 1985. Distribution of microtubules within the intestinal terminal web as revealed by quick-freezing and cryosubstitution. *Eur. J. Cell Biol.* 39:481-484.
51. Simons, K. 1987. Membrane traffic in an epithelial cell line derived from the dog kidney. *Kidney Int.* 32:S201-S207.
52. Spencer, R. P. 1961. Microvilli and intestinal surface area: an evaluation. *Gastroenterology.* 41:113-314.
53. Tsuchiya, S. 1981. Intracytoplasmic lumina of human breast cancer. *Acta. Pathol. Jpn.* 31:45-54.
54. Vale, R. D., J. M. Scholey, and M. P. Sheetz. 1986. Kinesin: possible biological roles for a new microtubule motor. *Trends Biochem. Sci.* 11:464-468.
55. Vallee, R. B., J. S. Wall, B. M. Paschal, and H. S. Shpetner. 1988. Microtubule-associated protein 1C from brain is a two-headed cytosolic dynein. *Nature (Lond.).* 332:561-563.
56. Vega-Salas, D. E., P. J. I. Salas, and E. Rodriguez-Boulan. 1987. Modulation of the expression of an apical plasma membrane protein of Madin-Darby canine kidney epithelial cells: cell-cell interactions control the appearance of a novel intracellular storage compartment. *J. Cell Biol.* 104:1249-1259.
57. Vega-Salas, D. E., P. J. I. Salas, and E. Rodriguez-Boulan. 1988. Exocytosis of vacuolar apical compartment (VAC): a cell-cell contact controlled mechanism for the establishment of the apical plasma membrane domain in epithelial cells. *J. Cell Biol.* 107:1717-1728.